[4]K. Krebs, Phys. Rev. 138, A143 (1965).
[5]P. Toya, J. Res. Inst. Catalysis, Hakkaido Univ. 6, 161 (1958); 6, 183 (1958).
[6]W. Cochran, *Inelastic Scattering of Neutrons* (International Atomic Energy Agency, Vienna, 1965), Vol. I.
[7]W. A. Harrison, *Pseudopotentials in the Theory of Metals* (Benjamin, New York, 1966).
[8]D. C. Wallace, Phys. Rev. 176, 832 (1968).
[9]A. J. Pinder and R. Pynn, J. Phys. C 2, 1037 (1969).
[10]D. Weaire, J. Phys. C 1, 210 (1968).
[11]T. Schneider and E. Stoll, *Neutron Inelastic Scattering* (International Atomic Energy Agency, Vienna, 1968), Vol. I, p. 211.
[12]V. Heine and I. V. Abarenkov, Phil. Mag. 9, 451 (1964).
[13]A. O. E. Animalu and V. Heine, Phil. Mag. 12, 1249 (1965).
[14]R. W. Shaw and W. A. Harrison, Phys. Rev. 163, 604 (1967).
[15]E. W. Kellerman, Phil. Trans. Roy. Soc. London A238, 573 (1940).
[16]P. P. Ewald, Ann. Physik, 64, 253 (1921).
[17]S. H. Vosko, Phys. Letters, 13, 97 (1964).
[18]J. C. Phillips and L. Kleinman, Phys. Rev. 128, 1437 (1962).
[19]J. Bardeen, Phys. Rev. 52, 688 (1937).
[20]J. Hubbard, Proc. Roy. Soc. (London) A243, 336 (1958).
[21]L. J. Sham, Proc. Roy. Soc. (London) A283, 33 (1965).
[22]D. J. W. Geldart and S. H. Vosko, Can. J. Phys. 44, 213 (1966).
[23]Paul S. Ho, Phys. Rev. 169, 523 (1968).

PHYSICAL REVIEW B VOLUME 2, NUMBER 10 15 NOVEMBER 1970

Effect of the Dielectric Function on the Phonon Spectrum of Magnesium†

Edward R. Floyd*
Department of Physics, University of Southern California, Los Angeles, California 90007
and
Leonard Kleinman
Department of Physics, University of Texas, Austin, Texas 78712
(Received 19 June 1970)

In this paper we demonstrate that an excellent fit to the phonon spectrum of a simple metal, magnesium, may be obtained with a local pseudopotential containing only two adjustable parameters. We compare the spectrum obtained with a fixed pseudopotential using different dielectric response functions. The Hubbard dielectric function yields phonon frequencies 30% greater than the Kleinman-Langreth one, with the random-phase approximation yielding intermediate frequencies.

I. INTRODUCTION

There have recently appeared a plethora of calculations of the phonon spectrum of magnesium. The first to appear, that of Roy and Venkataraman,[1] unfortunately contained errors in the secular determinant. Schneider and Stoll[2] obtained a nearly perfect fit to the experimental curves in the [0001] and [01$\bar{1}$0] wave-vector directions using a pseudopotential containing four adjustable parameters, whereas Brovman, Kagan, and Holas[3] needed to introduce, in addition to the pseudopotential, four short-range force constant parameters to obtain a good fit. Pindor and Pynn[4] used the optimized model potential (whose parameters are obtained by fitting the atomic spectra and not adjusted to fit the phonon spectrum) to obtain a poor fit to the phonon spectrum. Gilat, Rizzi, and Cubiotti[5] obtained a nearly perfect fit using the same method by arbitrarily replacing the electron mass with an effective mass $m^*=1.60m$. Shaw and Pynn,[6] taking exchange and correlation into account, effected a large improvement on the results of Pindor and Pynn[4] but still did not achieve a perfect fit to the experimental spectrum. Most recently, Prakash and Joski,[7] using a "first-principles" potential containing a Kohn-Sham[8] exchange potential screened by a procedure[9] we believe to be incorrect,[10] obtained a poor fit to the experimental phonon spectrum.

A secondary purpose of this paper is to demonstrate that a very good fit of phonon spectrum of magnesium can be obtained using a local pseudopotential containing only two adjustable parameters. When such a local pseudopotential is used, all exchange and correlation interactions between conduction electrons enter the calculation through the dielectric response function. It is the primary purpose of this paper to study the effect of various dielectric functions on the phonon dispersion curves. Because there is no way of knowing the "correct"

pseudopotential (or of calculating with sufficient accuracy a first-principles potential) we arbitrarily choose the pseudopotential to fit the phonon spectrum when the Kleinman-Langreth[11–13] dielectric function is used, and then using the same pseudopotential with the random-phase approximation (RPA) and Hubbard[14] dielectric functions, we recalculate the phonon spectrum. Thus we do not prove the superiority of ϵ_{KL} to ϵ_H or ϵ_{RPA} (that has been done elsewhere[11–13]) but merely demonstrate how sensitive the phonon spectrum is to the choice of ϵ.

II. PHONON SPECTRUM

The phonon spectrum $\omega(\vec{q})$ is obtained by solving the secular equation[15]

$$\det\{(M_b M_{b'})^{-1/2} E^{\alpha\beta}_{bb'}(\vec{q}) - \omega^2(\vec{q})\delta_{bb'}\delta_{\alpha\beta}\} = 0\,, \qquad (1)$$

with

$$E^{\alpha\beta}_{bb'}(\vec{q}) = \frac{1}{N}\sum_{mn}\frac{\partial^2 E}{\partial R^{\alpha}_{mb}\partial R^{\beta}_{nb'}}\, e^{-i\vec{q}\cdot(\vec{R}_m - \vec{R}_n)}\,, \qquad (2)$$

where $\vec{R}_m$ is a vector to the mth lattice point, $\vec{R}_{mb}$ is a vector to the bth atom in the mth cell, and the α, β superscripts indicate x, y, and z components. $E(\vec{R}_{mb})$ is the total ionic potential energy of the crystal including a direct ion-ion interaction energy plus the energy of the conduction electrons responding to the ionic potential. The former, $E^{\rm ion}$, is given by the Ewald-Fuchs formula.[16] The conduction electron contribution to $E(\vec{R}_{mb})$ is given by[17,18]

$$E^{\rm cond} = -\sum_{\kappa}(\Omega\kappa^2/16\pi\lambda)[1 - 1/\epsilon(\kappa)]\Big|\sum_{mb} V^I_{b\kappa} e^{-i\vec{\kappa}\cdot\vec{R}_{mb}}\Big|^2\,, \qquad (3)$$

where

$$V^I_{b\kappa} = (1/\Omega)\int V^I_b(\vec{r})\, e^{i\vec{\kappa}\cdot\vec{r}}\, d^3r\,. \qquad (4)$$

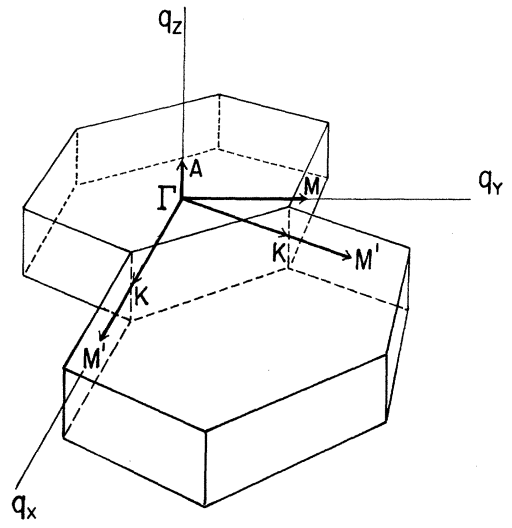

FIG. 1. Symmetry points in hexagonal Brillouin zone.

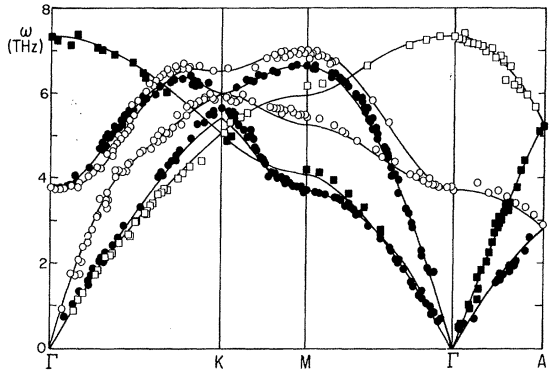

FIG. 2. Theoretical phonon dispersion curves (using ϵ_{KL}) and experimental data points (taken from Ref. 6).

Ω is the unit cell volume (two atomic cell volumes in hcp magnesium), N is the number of unit cells in the crystal, $\epsilon(\kappa)$ is the dielectric response function, and $V^I_b(\vec{r})$ is the ionic pseudopotential.[19] In the Appendix we compute $E^{\alpha\beta}_{bb'}(\vec{q})$ from $E^{\rm ion}$ and $E^{\rm cond}$.

We used an ionic pseudopotential of the form

$$V^I(\vec{r}) = -2Z(1+\gamma)/r - \sigma E_2[\int \varphi_{2sp}(r)\, d^3r]\,\varphi_{2sp}(r)\,, \qquad (5)$$

where φ_{2sp} is a parametrized Slater[20] magnesium core function

$$\varphi_{2sp} = \mathfrak{N}^{-1/2} r\, e^{-3.925\beta r} \qquad (6)$$

with $\mathfrak{N} = \int_0^\infty r^2 e^{-7.85\beta r} d^3r$ and E_2 is some average of $(E_{2s,2p} - E_{\rm cond})$. The parameters σ and β which are expected to be close to unity were chosen to be

$$\sigma = 3.9378/E_2\,, \quad \beta = 1.1725 \qquad (7)$$

in order to fit the phonon dispersion curves when $\epsilon_{KL}(\kappa)$ is used in Eq. (3). Since E_2 is about 6 Ry or less,[21] we see that σ and β are close to unity as expected.

$Z = 2$ is the valence charge of magnesium and γ, which represents the depletion hole (the charge missing from the plane-wave conduction electrons in the core region due to their orthogonalization to the core electrons), is given by

$$\gamma = \langle k|P|k\rangle_{\rm av}[1 - \langle k|P|k\rangle_{\rm av}]^{-1}\,, \qquad (8)$$

where P is the core projection operator and $\langle k|P|k\rangle_{\rm av} = 0.850$ for magnesium according to Harrison.[22]

The dielectric function $\epsilon_{KL}(\kappa, \omega = 0)$ is given by[11,13]

$$\epsilon_{KL}(\kappa) = 1 + \chi_1(\kappa)\left(1 - \frac{[B+A]\chi_1^2(\kappa) + [B-A]\chi_2^2(\kappa)}{2\chi_1(\kappa)}\right)^{-1}\,, \qquad (9)$$

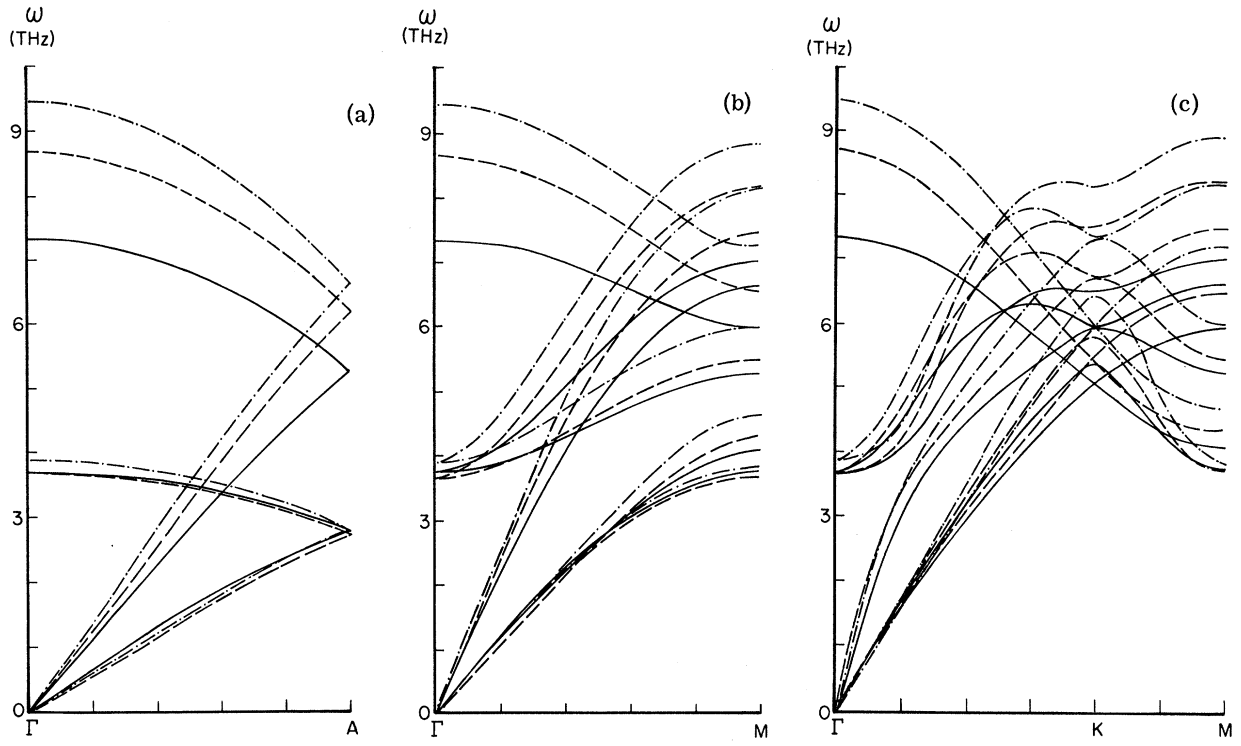

FIG. 3. Comparison of phonon dispersion curves in three directions obtained using ϵ_{RPA}(dashed), ϵ_{H}(dots and dashes), and ϵ_{KL}(solid lines).

$$A = \tfrac{1}{2}\kappa^2/(2\alpha k_f^2 + K_s^2), \tag{10}$$

$$B = \tfrac{1}{2}\kappa^2/(2\alpha k_f^2 + \kappa^2 + K_s^2), \tag{11}$$

$$\chi_1(\kappa) = \frac{2(1+\gamma)^2}{\pi\kappa^3}\left[k_f^2 - \left(\frac{\kappa^2+\Delta(\kappa)}{2\kappa}\right)^2 \times \ln\left|\frac{\kappa^2+\Delta(\kappa)+2\kappa k_f}{\kappa^2+\Delta(\kappa)-2\kappa k_f}\right| + \frac{k_f}{\kappa}\left(\kappa^2+\Delta(\kappa)\right)\right], \tag{12}$$

$$\chi_2(\kappa) = \frac{2(1+\gamma)^2}{\kappa^3}\left[k_f^2 - \left(\frac{\kappa^2+\Delta(\kappa)}{2\kappa}\right)^2\right] \quad \text{if } \Delta(\kappa) < 2\kappa k_f - \kappa^2$$

$$= 0, \quad \text{otherwise} \tag{13}$$

$$\Delta(\kappa) = (4/3\pi)\, k_f^3 [\kappa^2/(2\alpha k_f + \kappa^2 + K_s^2)(2\alpha k_f^2 + K_s^2)], \tag{14}$$

$$\alpha = \tfrac{1}{2}(1 + e^{-\kappa/2k_f}), \tag{15}$$

and the Thomas-Fermi value of the screening constant is taken, $K_s^2 = 4k_f/\pi$.

The calculation was performed using lattice constants[17,23] $a = 6.026$ and $c = 9.784$. We used 681 reciprocal lattice vectors in the sums (A4)–(A7) which roughly form a spheroid in $\vec{k}$ space of radius $7k_f$ in the base plane and $6k_f$ along the z axis. This choice was made to compensate for the fact that the Brillouin zone has larger dimensions in the base plane. For $\vec{q} = 0$ there is much cancellation within each set of reciprocal lattice vectors in the sums (A4)–(A7) and the convergence is rapid. As $\vec{q}$ gets large and the various $(\vec{G}+\vec{q})$ have different magnitude, the cancellation within each set of reciprocal lattice vectors disappears and the convergence becomes poor. We chose the Ewald convergence factor in (A2)–(A5) to be $\eta = 4/a$. With this choice, the contributions of (A2) and (A3) could be completely neglected while (A4) and (A5) were still better converged than the conduction electron contributions (A6) and (A7). The phonon spectrum was calculated for $\vec{q}$ vectors along the symmetry directions ΓK, ΓM, MK, and ΓA shown in Fig. 1. In Fig. 2 we show the spectrum along with the experimental data.[24,25] We have not made any correction for the lack of convenience in the sums (A4)–(A7) as the parameters in Eq. (7) were chosen to give the best fit to the experimental data for the 681 reciprocal lattice vector expansion.

We have studied the convergence properties of the calculation in the following manner. We have calculated the eigenfrequencies at the equivalent points M and M' (see Fig. 1). Because $|\vec{q}_{M'}| = \sqrt{3}\,|\vec{q}_M|$, the convergence at M' is much worse than at M and considerable difference exists between the calculated

TABLE I. Calculated frequencies (in THz) at equivalen points M and M' without and with convergence correction.

M	M'	M_{conv}	M'_{conv}
M_4^+ 3.76	4.14	3.67	3.67
M_3^+ 4.15	4.58	3.90	3.93
M_3^- 5.25	5.52	5.19	5.18
M_4^- 6.01	6.28	5.87	5.79
M_2^- 6.63	6.68	6.54	6.54
M_1^+ 6.98	7.03	6.89	6.89

values in Table I. Now because of time reversal symmetry, ω^2 may be expanded in powers of q^2 and so may $\delta\omega^2$, the convergence error. If we assume perfect convergence at $q=0$ and drop all higher powers of q^2 we have

$$\delta\omega^2_{\vec{q}p} = b_{\vec{q}p} q^2 , \tag{16}$$

where the subscript p indicates the phonon mode and the subscript $\vec{q}$ indicates that $b_{\vec{q}p}$ is a function of the direction of the $\vec{q}$ vector though not of its magnitude. Because of a σ_y reflection plane, the dispersion curves along q_y must be symmetrical about M. By adding $\delta\omega^2$ to the calculated frequencies at two q_y points equidistant from M, one may determine what value of $b_{\vec{q}}$ is needed to make the two frequencies equal. Then

$$M_{p\,\text{conv}} = M_p + b_{Mp} q_M^2 . \tag{17}$$

A similar procedure was carried out for the M' point using the σ_x reflection plane. M_{conv} and M'_{conv} are listed in Table I; the agreement is perfect for modes vibrating in the xy plane and quite good for the z modes.

Using the same pseudopotential parameters [Eq. (7)], we have calculated the phonon curves replacing ϵ_{KL} by ϵ_{RPA} and ϵ_H, where

$$\epsilon_{RPA}(\kappa) = 1 + \chi_{10}(\kappa) , \tag{18}$$

$$\epsilon_H = 1 + \chi_{10}(\kappa)[1 - A\chi_{10}(\kappa)]^{-1} , \tag{19}$$

where χ_{10} is given by Eq. (12) with Δ set equal to zero and A is given in Eq. (10). The Thomas-Fermi value was again used for K_s^2 but Hubbard's[14] choice of $\alpha = \frac{1}{2}$ was used instead of Eq. (15).[26] The dispersion curves for the three dielectric functions are compared in Fig. 3. These emphasize the sensitivity of the phonon dispersion curves to the choice of dielectric function. It is interesting to note that even though they give very similar corrections to the RPA pair distribution function,[13] ϵ_H and ϵ_{KL} cause changes in the RPA phonon dispersion curves of opposite sign.

It is interesting to note that the exchange corrected dispersion curves of Shaw and Pynn[6] lie below their RPA dispersion curves. For large wave vector their exchange correction becomes just Hubbard's. We, on the other hand, have found the Hubbard exchange corrected dispersion curves to lie above the RPA. The reason for this is quite simple. Shaw and Pynn use an *atomic* model potential[27] which presumably contains all exchange and correlation corrections to the potential. Their RPA result then subtracts off half the direct Coulomb conduction-electron–conduction-electron interaction but no exchange while their Hubbard result subtracts off half the Coulomb and half the Hubbard exchange interactions. We, however use an *ionic* pseudopotential and add half the Coulomb and Hubbard exchange contributions. Presumably, had Shaw and Pynn used the KL exchange correction, they would have obtained dispersion curves lying above their RPA dispersion curves, again opposite to our result. The use of an atomic model potential seems inappropriate to us in view of the fact that there is no exchange between the valence electrons in the ground state of atomic Mg.

APPENDIX

We here calculate $E_{bb'}^{\alpha\beta}(q)$ from Eq. (2). The Ewald-Fuchs[16] formula for the energy of a crystal consisting of positive point ions[28] sitting in a constant background of negative charge may be written[17]

$$E^{\text{ion}} = Z^{*2}\left(\frac{-4\pi N}{\Omega\eta^2} - \frac{4\eta N}{\pi} + \sum_{nb\neq mb'} \frac{F(\eta|\vec{R}_{nb} - \vec{R}_{mb'}|)}{|\vec{R}_{nb} - \vec{R}_{mb'}|}\right.$$

$$\left. + \frac{4\pi}{N\Omega} \sum_{nbmb'\kappa} e^{i\vec{\kappa}\cdot(\vec{R}_{nb} - \vec{R}_{mb'})} e^{-\kappa^2/4\eta^2} \kappa^{-2}\right), \tag{A1}$$

where $Z^* = (1+\gamma)Z$ and

$$F(x) = (2/\sqrt{\pi}) \int_x^\infty e^{-y^2} dy .$$

Substituting the third term of Eq. (A1) into Eq. (2) we obtain

$$[E_{bb}^{\alpha\beta}(q)]^{\text{ion I}} = 2Z^{*2} \sum_n{}' \cos\vec{q}\cdot\vec{R}_n \left[\frac{\delta_{\alpha\beta}}{R_n^2}\left(\frac{F(\eta R_n)}{R_n} + \frac{2\eta}{\sqrt{\pi}} e^{-\eta^2 R_n^2}\right) - \frac{R_n^\alpha R_n^\beta}{R_n^2}\left(\frac{3F(\eta R_n)}{R_n^3} + \frac{6\eta}{\sqrt{\pi}} \frac{e^{-\eta^2 R_n^2}}{R_n^2} + \frac{4\eta^3}{\sqrt{\pi}} e^{-\eta^2 R_n^2}\right)\right]$$

$$+ 2Z^{*2} \sum_{nb'}{}' \left[\frac{-\delta_{\alpha\beta}}{R_{nb'}^2}\left(\frac{F(\eta R_{nb'})}{R_{nb'}} + \frac{2\eta}{\sqrt{\pi}} e^{-\eta^2 R_{nb'}^2}\right) + \frac{R_{nb'}^\alpha R_{nb'}^\beta}{R_{nb'}^2}\left(\frac{3F(\eta R_{nb'})}{R_{nb'}^3} + \frac{6\eta}{\sqrt{\pi}} \frac{e^{-\eta^2 R_{nb'}^2}}{R_{nb'}^2} + \frac{4\eta^3}{\sqrt{\pi}} e^{-\eta^2 R_{nb'}^2}\right)\right], \tag{A2}$$

$$[E_{bb'}^{\alpha\beta}(\vec{q})]^{\text{ion I}} = 2Z^{*2}\sum_n e^{i\vec{q}\cdot\vec{R}_n}\left[\frac{\delta_{\alpha\beta}}{R_{nb'b}^2}\left(\frac{F(\eta R_{nb'b})}{R_{nb'b}} + \frac{2\eta}{\sqrt{\pi}}\, e^{-\eta^2 R_{nb'b}^2}\right)\right.$$

$$\left. - \frac{R_{nb'b}^{\alpha} R_{nb'b}^{\beta}}{R_{nb'b}^2}\left(\frac{3F(\eta R_{nb'b})}{R_{nb'b}^3} + \frac{6\eta}{\sqrt{\pi}}\,\frac{e^{-\eta^2 R_{nb'b}^2}}{R_{nb'b}^2} + \frac{4\eta^3}{\sqrt{\pi}}\, e^{-\eta^2 R_{nb'b}^2}\right)\right], \tag{A3}$$

where $R_{nb'b} = |\vec{R}_{0b} - \vec{R}_{nb'}|$ and we have used

$$\sum_{nm} f(|\vec{R}_{mb} - \vec{R}_{nb'}|) = N\sum_n f(R_{nb'b}).$$

Substituting the last term of (A1) into (2) yields

$$[E_{bb}^{\alpha\beta}(\vec{q})]^{\text{ion II}} = \frac{8\pi Z^{*2}}{\Omega}\left(\sum_{\vec{G}} \frac{(G+q)^{\alpha}(G+q)^{\beta}}{|\vec{G}+\vec{q}|^2}\, e^{-(\vec{G}+\vec{q})^2/4\eta^2} - \sum_{\vec{G}b'} \frac{G^{\alpha}G^{\beta}}{G^2}\, e^{-G^2/4\eta^2}\,\tfrac{1}{2}(e^{i\vec{G}\cdot\vec{R}_{0b'}} + e^{-i\vec{G}\cdot\vec{R}_{0b'}})\right), \tag{A4}$$

$$[E_{bb'}^{\alpha\beta}(\vec{q})]^{\text{ion II}} = \frac{8\pi Z^{*2}}{\Omega}\sum_{\vec{G}} \frac{(G+q)^{\alpha}(G+q)^{\beta}}{|\vec{G}+\vec{q}|^2}\, e^{-(G+q)^2/4\eta^2}\, e^{i(\vec{G}+\vec{q})\cdot(\vec{R}_{0b}-\vec{R}_{0b'})}, \tag{A5}$$

where the $\vec{G}$ are reciprocal lattice vectors and we have used

$$\sum_{nm} e^{i(\vec{k}-\vec{q})\cdot(\vec{R}_n-\vec{R}_m)} = N^2\delta_{\vec{G},\vec{k}-\vec{q}}\ .$$

Finally, substituting Eq. (3) into Eq. (2) we obtain

$$[E_{bb}^{\alpha\beta}(\vec{q})]^{\text{cond}} = \frac{-\Omega}{8\pi}\sum_{\vec{G}} (\vec{G}+\vec{q})^2\left(1 - \frac{1}{\epsilon(\vec{G}+\vec{q})}\right)|V_{\vec{G}+\vec{q}}^{I}|^2 (G+q)^{\alpha}(G+q)^{\beta}$$

$$+ \frac{\Omega}{16\pi}\sum_{Gb'} G^2\left(1 - \frac{1}{\epsilon(G)}\right)|V_G^I|^2 G^{\alpha}G^{\beta}(e^{i\vec{G}\cdot\vec{R}_{0b'}} + e^{-i\vec{G}\cdot\vec{R}_{0b'}}), \tag{A6}$$

$$[E_{bb'}^{\alpha\beta}(\vec{q})]^{\text{cond}} = \frac{-\Omega}{8\pi}\sum_{\vec{G}} (\vec{G}+\vec{q})^2\left(1 - \frac{1}{\epsilon(\vec{G}+\vec{q})}\right)|V_{\vec{G}+\vec{q}}^{I}|^2 (G+q)^{\alpha}(G+q)^{\beta} e^{i(\vec{G}+\vec{q})\cdot(\vec{R}_{0b}-\vec{R}_{0b'})}. \tag{A7}$$

Note that in the $G \to 0$ limit $V_G^I \to 8\pi Z^*/\Omega G^2$ and $[1 - 1/\epsilon(G)] \to 1$ so that the second term of (A6) cancels the second term of (A4). Note also that for the hcp structure

$$E_{bb'}^{\alpha\beta}(q) = E_{b'b}^{\alpha\beta}(q)^*.$$

Finally we note that our dynamical matrix differs from Gilat *et al.*[5] in two respects aside from a factor of 2 due to our use of Rydberg atomic units. Our Eq. (2) has a phase factor $\vec{q}\cdot(\vec{R}_m - \vec{R}_n)$ rather than $\vec{q}\cdot(\vec{R}_{mb} - \vec{R}_{nb'})$ leading to a factor of $e^{i\vec{q}\cdot(\vec{R}_{0b}-\vec{R}_{0b'})}$ in all bb' matrix elements and we have not subtracted

$$\sum_{nb'} \frac{\partial^2 E}{\partial R_{mb}^{\alpha}\partial R_{nb'}^{\beta}} = 0$$

from our matrix as they have.

†Research sponsored by the U. S. Air Force Office of Scientific Research Office of Aerospace Research, under Grant No. AFOSR 68-1507.

*Present address: Naval Undersea Research and Development Center, San Diego, Calif.

[1]A. P. Roy and G. Venkataraman, Phys. Rev. 156, 769 (1967).

[2]T. Schneider and E. Stoll, *Neutron Inelastic Scattering* (International Atomic Energy Agency, Vienna, 1968), Vol. I, p. 101.

[3]E. G. Brouman, Yu. Kagan, and A. Holas, *Neutron Inelastic Scattering* (International Atomic Energy Agency, Vienna, 1968), Vol. I, p. 165.

[4]A. Pindor and R. Pynn, J. Phys. C 2, 1037 (1969).

[5]G. Gilat, G. Rizzi, and G. Cubiotti, Phys. Rev. 185, 971 (1969).

[6]R. W. Shaw, Jr. and R. Pynn, J. Phys. C 2, 2071 (1969).

[7]S. Prakash and S. K. Joshi, Phys. Rev. B 1, 1468 (1970).

[8]W. Kohn and L. J. Sham, Phys. Rev. 140, A1133 (1965).

[9]J. E. Robinson, F. Bassani, R. S. Knox, and J. R.

Schrieffer, Phys. Rev. Letters 9, 215 (1962).
[10]J. C. Phillips and L. Kleinman, Phys. Rev. 128, 2098 (1962). (See the note added in proof.)
[11]L. Kleinman, Phys. Rev. 172, 383 (1968).
[12]D. C. Langreth, Phys. Rev. 181, 753 (1969).
[13]P. R. Antoniewicz and L. Kleinmann Phys. Rev. B 2, (1970).
[14]J. Hubbard, Proc. Roy. Soc. (London) A243, 336 (1957).
[15]J. M. Ziman, *Electrons and Phonons* (Oxford U. P., London, 1963), Eq. (1.6.13).
[16]K. Fuchs, Proc. Roy. Soc. (London) A151, 585 (1935).
[17]We use Rydberg atomic units throughout this paper except in Eq. (1), where we convert to cgs units.
[18]This formula is equivalent to Eq. (8-99) in Ref. 22. Note that ϵ here is the true "test charge" dielectric function. In terms of the electron dielectric function (inverse vertex function) $(1-1/\epsilon)=\chi_1/\epsilon_e$. See Eqs. (13) and (30) of Ref. 11.
[19]J. C. Phillips and L. Kleinman, Phys. Rev. 116, 287 (1959).
[20]J. C. Slater, Phys. Rev. 42, 33 (1932).
[21]F. Herman and S. Skillman, *Atomic Structure Calculations* (Prentice Hall, Englewood Cliffs, N. J., 1963).
[22]W. A. Harrison, *Pseudopotentials in the Theory of Metals* (Benjamin, New York, 1966), p. 40.
[23]L. Falicov, Proc. Roy. Soc. (London) A255, 47 (1962).
[24]R. Pynn and G. L. Squires, *Neutron Inelastic Scattering* (International Atomic Energy Agency, Vienna, 1968), Vol. I, p. 215.
[25]P. K. Iyengar, G. Venkataraman, P. R. Vijayaraghavan, and A. P. Roy, *Inelastic Scattering Neutrons in Solids and Liquids* (International Atomic Energy Agency, Vienna, 1965), Vol. I, p. 153.
[26]With α given by Eq. (15) in ϵ_H, the discrepancy between the Hubbard and Kleinman-Langreth dispersion curves becomes even larger than that shown in Fig. 3.
[27]R. W. Shaw, Jr., J. Phys. C 2, 2335 (1969) [see Eq. (1)].
[28]The fact that our ions are not point ions does not concern us because it only adds a constant ($\vec{R}_{mb}$ independent) term to Eq. (A1).

PHYSICAL REVIEW B VOLUME 2, NUMBER 10 15 NOVEMBER 1970

Temperature Dependence of the Elastic Constants

Y. P. Varshni
Department of Physics, University of Ottawa, Ottawa 2, Canada
(Received 4 May 1970)

The following two equations are proposed for the temperature dependence of the elastic stiffness constants: $c_{ij}=c_{ij}^0-s/(e^{t/T}-1)$ and $c_{ij}=a-bT^2/(T+c)$, where c_{ij}^0, s, t, a, b, and c are constants. The applicability of these two equations and that of Wachtman's equation is examined for 57 elastic constants of 22 substances. The first equation has a theoretical justification and gives the best over-all results. Neither of the three equations give the theoretically expected T^4 dependence at low temperatures, and therefore they are not expected to give very accurate results at very low temperatures ($\lesssim\Theta_D/50$). A new melting criterion is also examined.

I. INTRODUCTION

The theory of the temperature dependence of the elastic constants was first developed by Born and co-workers.[1] In this theory, the temperature dependence of the elastic constants arises from the variation of the lattice potential energy due to anharmonicity. In the limiting cases, the theory[1,2] shows that the lattice contribution to $c_{ij}(T)-c_{ij}(0)$ should vary as T^4 at very low temperatures and as T at high temperatures. Here c_{ij} represents an elastic stiffness constant.

During the last two decades the variation of the elastic constants with temperature has been measured for a large number of substances. On the experimental side, in Fig. 1, we show a typical set of data. The general pattern conforms to theoretical expectation. However, the T^4 dependence at low temperatures has not yet been unambiguously established; the scanty evidence which is available appears to indicate that its range of validity is rather small. Further, some metallic substances have been found[3-5] to show a T^2 dependence at low temperatures. Bernstein[6] has shown that such a dependence can arise from the temperature dependence of the electron energy due to the Fermi-Dirac distribution of electrons.

We may note here that there are many substances whose one or more elastic stiffness constants do not show the type of behavior shown in Fig. 1 (e.g., see figures in Hearmon[7]). In the present paper we shall not consider such elastic constants, but confine ourselves to those that show the regular behavior typified in Fig. 1.

Attempts have been made to represent the temperature dependence of elastic constants by empirical equations. We quote here three of these.

Sutton[8] was able to represent the variation of c_{44} of aluminum over the range 63–773 °K with an accuracy better than $\frac{1}{2}\%$ by the following equation: